Received: 21 March 2022 | Revised: 5 May 2022 | Accepted: 18 May 2022

DOI: 10.1002/jcla.24528

RESEARCH ARTICLE

WILEY

Circular RNA hsa_circ_0043688 serves as a competing endogenous RNA for microRNA-145-5p to promote the progression of Keloids via Fibroblast growth factor-2

Ye Liu | Xin Wang | Ziqiao Ni | Yinqiu Li | Jiaqian Song | Fei Zhu | Xiaojing li

Department of Plastic Surgery, The First Affiliated Hospital of Anhui Medical University, Hefei, China

Correspondence
Fei Zhu and Xiaojing Li, Department of Plastic Surgery, The First Affiliated Hospital of Anhui Medical University, No, 218, Jixi Road, Hefei 230061, China.
Emails: feizhu1234560427@163.com; 63610407@qq.com

Funding information
This study was supported by regulation of the inflammation by TSG-6 and its mechanism in pathological scar (No. 81272107) and the Key Science and Technology Project of Anhui Province (No. 1604a0802078).

Abstract

Background: Keloids are benign fibroproliferative skin tumors. Circular RNA (circRNA) hsa_circ_0043688 has been exhibited to the freakishly expressed in keloid tissues. Here, we aimed to investigate the regulatory network of hsa_circ_0043688 in the pathological process of keloid.

Methods: Hsa_circ_0043688, microRNA-145-5p (miR-145-5p), and Fibroblast growth factor-2 (FGF2) level were detected using RT-qPCR. Cell viability, proliferation, apoptosis, invasion, and migration were investigated using Cell Counting Kit-8 (CCK-8), 5-ethynyl-2′-deoxyuridine (EdU), flow cytometry, transwell, and wound healing assays, respectively. Western blot analysis of protein levels of FGF2, CyclinD1, Collagen I, and Collagen III. After the prediction of Circinteractome and Starbase, their interaction was verified based on a dual-luciferase reporter and RIP assays.

Results: Increased hsa_circ_0043688 and FGF2, and decreased miR-145-5p in keloids samples and fibroblasts were found. Also, hsa_circ_0043688 absence hindered proliferation, invasion, migration, and boost apoptosis of keloid fibroblasts. In mechanism, hsa_circ_0043688 modulated FGF2 content via sponging miR-145-5p.

Conclusion: Hsa_circ_0043688 knockdown inhibited cell growth and metastasis of keloid fibroblasts via miR-145-5p/FGF2, providing a new mechanism to understand the keloid progression.

KEYWORDS
FGF2, Hsa_circ_0043688, keloid fibroblasts, miR-145-5p, proliferation

1 | INTRODUCTION

As a fibroproliferative dermal tumor, keloids, occur as a result of aberrant wound healing processes in predisposed individuals.[1,2] Keloid tissues grow beyond and above the margins of the original wound and are pathologically characterized by aggressive fibroblasts growth, and excessive extracellular matrix (ECM) deposition.[3,4] Owing to pain, itching, and aesthetic impairment, keloids can cause huge physical, emotional and psychological distress for patients.[5,6] Currently, conventional treatments, containing surgical excision, cryotherapy, and laser therapy, have been reported to be beneficial, but keloid recurrence frequently occurs.[7,8] Accordingly, understanding the mechanism underlying keloid formation is highly desirable for developing better treatment approaches.

Over the past several years, increasing research has focused on unraveling the importance of numerous large non-coding RNAs, which are transcribed by >90% of the mammalian genome.[9,10] Circular RNAs (circRNAs) can be divided into non-coding RNAs and coding circRNAs.[11] In fact, circRNAs represent a distinct group of covalently closed RNA molecules that derive from back splicing events of pre-mRNA transcripts.[12,13] Since their remarkable abundance, high stability, and wide distribution, circRNAs exhibit a potential attractive biomarker in a variety of diseases.[14,15] Much laboratory work discovered circRNAs are being found correlated with the development of various human diseases, including keloid.[16] For instance, Lv et al. indicated that circCOL5A1 could exacerbate the pathological hyperplasia of keloids by boosting proliferation, migration, and ECM deposition.[17] Likewise, Yang et al. conjectured that the deficiency of circ_101238 tended to repress the progression of keloid formation via acting upon the downstream the miR-138-5p/cyclin-dependent kinase 6 (CD6).[18] Of note, hsa_circ_0043688, a typical circRNA originating from the FK506-binding protein 10 (FKBP10) gene, has been recently documented to be increased in keloid tissues.[19] Nonetheless, the functional role of hsa_circ_0043688 in specific steps of keloid formation is still unknown.

Nowadays, some scholars painted out circRNAs could perform as the ceRNAs through sequestering particular microRNAs response elements (MREs) to regulate gene transcription.[20,21] Furthermore, hsa_circ_0043688 was conjectured to participate in the modulation of keloid pathogenesis by the circRNA-miRNA interaction network in a previous study.[19] Herein, hsa_circ_0043688 possessed miR-145-5p binding sites in keloid fibroblasts. Meanwhile, a microarray data analysis presented a downregulated miR-145-5p in keloid fibroblasts.[22] Thus, the purpose of this article is to preliminarily investigate hsa_circ_0043688's regulatory network with miR-145-5p in keloid formation.

2 | MATERIALS AND METHODS

2.1 | Clinical samples and cell culture

Fifty-one fresh keloid tissues and matched normal skin tissues were collected after signing written informed consent from each patient recruited at the First Affiliated Hospital of Anhui Medical University. Meanwhile, approval from the Ethics Committee of the First Affiliated Hospital of Anhui Medical University was obtained.

Based on the previous description, primary fibroblasts were isolated from the collected skin and keloid tissue samples. In general, these samples were treated with PBS, followed by removing the epidermis and subcutaneous adipose. After cutting into 0.5 cm^3 pieces, the samples were digested, filtered, and centrifuged at 500*g* for 10 min. Finally, the collected fibroblasts were grown in Dulbecco's modified Eagle's Medium (Invitrogen, Paisley Scotland, UK). Also, supplements containing 10% fetal bovine serum (FBS; PAN Biotech, Aidenbach, Germany) and 1% penicillin/streptomycin (PAN Biotech) were added into the culture medium at 37°C in 5% CO_2. Then, cells of fibroblasts in passages 3 to 5 were selected for the following assays. For confirming the stability of hsa_circ_0043688, keloid fibroblasts were treated with 3 U/μg of RNase R for 30 min.

TABLE 1 The sequences of primers for RT-qPCR used in this study

Names	Sequences (5′-3′)
Hsa_circ_0043688: Forward	TTTGTGTGGCACAAGGACCC
Hsa_circ_0043688: Reverse	GCCCTTACT GTAGCTCCTCCG
Linear FKBP10: Forward	GACCTGCAATGAGACCACCA
Linear FKBP10: Reverse	CCGTAGTCATGCGAGGTGAA
miR-145-5p: Forward	GTCCAGTTTTCCCAGGA
miR-145-5p: Reverse	GAACATGTCTGCGTATCTC
FGF2: Forward	GGGGTTGTGTCTATCAAAGGAG
FGF2: Reverse	GTGCCACATACCAACTGGAGTA
U6: Forward	CTCGCTTCGGCAGCACA
U6: Reverse	AACGCTTCACGAATTTGCGT
GAPDH: Forward	GGTCACCAGGGCTGCTTT
GAPDH: Reverse	GGAAGATGGTGATGGGATT

2.2 | RT-qPCR

After being treated using TRIzol reagent (Invitrogen), the prepared total RNA was processed with PrimeScript™ RT Master Mix (TaKaRa, Shiga, Japan). After that, quantitative real-time PCR for gene expression was implemented with an SYBR Green PCR Kit (TaKaRa) using an ABI 7900 detection System (Applied Biosystems, Warrington, UK). In the end, the obtained data were analyzed in the light of the $2^{-\Delta\Delta Ct}$ method, normalizing with GAPDH and U6. Also, the primer required was presented in Table 1.

2.3 | Subcellular fractionation assay

After being isolated nuclear and cytoplasmic RNA from keloid fibroblasts using PARIS kit, hsa_circ_0043688 content in the cytoplasmic section and nuclear section was detected using RT-qPCR assay.

2.4 | Cell transfection

Hsa_circ_0043688 small interference RNA (si-hsa_circ_0043688), miR-145-5p mimic/inhibitor (miR-145-5p/anti-miR-145-5p), and the corresponding controls (si-NC, miR-NC, anti-miR-NC) were acquired from RiboBio (Guangzhou, China). Also, a pcDNA-fibroblast growth factor 2 (FGF2) vector was established using a pcDNA (GenePharma, Shanghai, China). Then 20 nM of oligonucleotides and 50 ng of vectors were transiently transfected into keloid fibroblasts using

Lipofectamine 3000 (Invitrogen). Hsa_circ_0043688 sequence was cloned into the pCD5 vector to generate the pCD5-hsa_circ_0043688 plasmid (hsa_circ_0043688, Geneseed, Guangzhou, China).

2.5 | Cell viability assay

Keloid fibroblasts were introduced into 96-well plates with 2×10^3 cells/well. After mixing the cell counting kit (CCK-8) solution (10 μl, Dojindo, Kumamoto, Japan) for 4 h, cell viability was analyzed using a microplate reader.

2.6 | 5-ethynyl-2′-deoxyuridine (EdU) assay

In brief, 5×10^4 transfected keloid fibroblasts in 6-well plates were incubated with 50 μM EdU (RiboBio). After fixation, the cells were stained with Apollo Dye Solution and DAPI, followed by visualization using a fluorescence microscope.

2.7 | Cell apoptosis assay

Generally, transfected keloid fibroblasts were pelleted and washed, followed by re-suspending in a binding buffer containing 5 μl Annexin (V-fluorescein isothiocyanate) V-FITC and 10 μl Propidium iodide (PI) (Roche, Indianapolis, IN, USA) for 15 min. Referring to the operation manual of flow cytometry (BD Biosciences, Heidelberg, Germany), the keloid fibroblast apoptosis rates were analyzed.

2.8 | Transwell assay

Briefly, 1×10^5 transfected keloid fibroblasts in a serum-free medium were plated in the top chamber (Corning Costar, Corning, NY, USA) with the matrigel-coated membrane (BD Biosciences), and the medium supplemented with serum was introduced into the lower counterparts. Whereafter, the cells were incubated for 24 h, and cells on the lower surface of the membrane were stained with 0.1% crystal violet (Sigma-Aldrich, St. Louis, MO, USA). At length, the cells were figured out using a microscope (Nikon, magnification ×100).

2.9 | Wound healing assay

In 6-well plates, transfected keloid fibroblasts were grown to 90–95% confluence, followed by scratching the monolayer using a pipette tip. After creating a cell-free area, the cell debris was removed and the photos of the wounds (time 0 h) were taken. After incubation for 24 h in a serum-free medium, a microscope and Image J software were used to analyze the migration ability.

2.10 | Western blot assay

Lysis of cells and tissue was prepared using RIPA buffer (Sigma-Aldrich). After being separated by 10% SDS-PAGE and transferred to nitrocellulose membranes, the blot was probed with primary antibodies: CyclinD1 (1:1000, ab40754), Collagen I (1:1000, ab34710), Collagen III (15,000, ab7778), FGF2 (11,000, ab92337), and the secondary antibody (ab6721, 1:10000). Also, these antibodies were obtained from Abcam (Cambridge, MA, USA). The blots were detected in light of an ECL detection kit (GE Healthcare UK Ltd, Little Chalfont, UK).

2.11 | Dual-luciferase reporter assay

In short, wild-type (WT) constructs (WT-hsa_circ_0043688 or WT-FGF2 3'UTR) and the site-directed mutant (MUT) constructs in the seed sequence (MUT-hsa_circ_0043688 or MUT-FGF2 3'UTR) were purchased from Hanbio (Shanghai, China). After being transfected into keloid fibroblasts with a luciferase reporter construct and miR-145-5p or miR-NC for 48 h, an assessment of luciferase activities was carried out, in line with a dual-luciferase reporter assay kit.

2.12 | RNA immunoprecipitation

In this assay, keloid fibroblasts at 80% confluency were harvested, followed by lysis in complete 2.12. RNA immunoprecipitation (RIP) lysis buffer (Millipore). After co-immunoprecipitated with magnetic beads containing anti-Ago2 or anti-IgG antibody, the samples were digested with proteinase K and subjected to RT-qPCR analysis.

2.13 | Statistical analysis

Expression association was implemented by Pearson correlation analysis. Data were given as mean ± standard deviation (SD). Statistical differences were operated by Student's *t*-test or one-way analysis of variance (ANOVA) with Tukey's test. All statistical analyses were executed according to GraphPad Prism7 (GraphPad software, San Diego, CA, USA). There was a statistically significant difference when $p<0.05$.

3 | RESULTS

3.1 | Hsa_circ_0043688 expression was increased in keloid tissues and fibroblasts

To begin with, we investigated the expression level of hsa_circ_0043688 in human keloid tissues ($n = 51$) and corresponding adjacent normal skin tissues ($n = 51$) from keloid patients. As shown in Figure 1A, the significant upregulation of hsa_circ_0043688

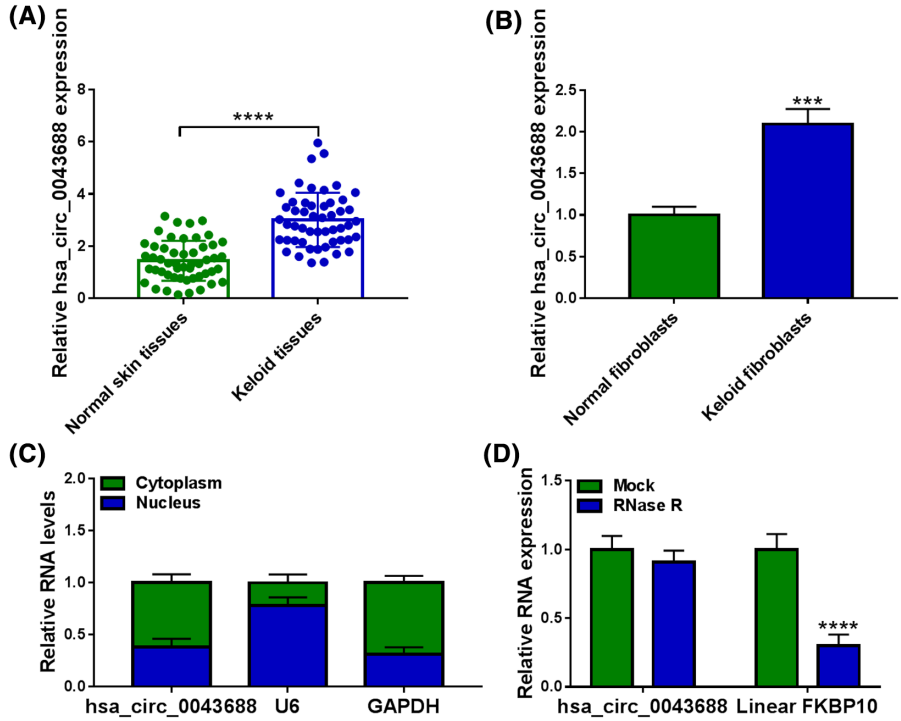

FIGURE 1 Hsa_circ_0043688 expression in keloid. (A and B) RT-qPCR analysis of hsa_circ_0043688 content in 51 normal skin tissues, 51 keloid tissues, normal fibroblasts, and keloid fibroblasts. (C) Subcellular fractionation analysis of hsa_circ_0043688 cellular localization in keloid fibroblasts. (D) Effects of RNase R treatment on hsa_circ_0043688 and linear FKBP10 in keloid fibroblasts. ***$p < 0.001$, ****$p < 0.0001$

was viewed in keloid tissue samples. Moreover, we further verified that hsa_circ_0043688 was overtly overexpressed in keloid fibroblasts when compared with normal fibroblasts (Figure 1B). Also, hsa_circ_0043688 was predominantly located in the cytoplasm of keloid fibroblasts (Figure 1C). Then, keloid fibroblasts were treated with RNase R. Data suggested that the circular isoform was resistant to RNase R (Figure 1D). Overall, hsa_circ_0043688 dysregulation might be related to the keloid development.

3.2 | Knockdown of hsa_circ_0043688 blocked proliferation, invasion, migration, and expedited apoptosis in keloid fibroblasts

Then, the loss-of-function of hsa_circ_0043688 was carried out in keloid fibroblasts for the biological functions of hsa_circ_0043688. As presented in Figure 2A, we first used RNA interference to silence hsa_circ_0043688 content, and the knockdown efficiency of hsa_circ_0043688 was detected by RT-qPCR assay. Whereafter, cell viability was markedly reduced in keloid fibroblasts by hsa_circ_0043688 downregulation relative to the negative controls (Figure 2B). In parallel, EdU assay exhibited hsa_circ_0043688 absence obviously reduced EdU-positive keloid fibroblasts number in comparison with that of control si-NC (Figure 2C). Besides, an enhanced apoptosis rate of keloid fibroblasts was observed due to the deficiency of hsa_circ_0043688 (Figure 2D). Apart from that, the introduction of si-hsa_circ_0043688 caused significant suppression of cell invasion (Figure 2E) and migration (Figure 2F) in keloid fibroblasts compared to that of the corresponding control groups. Subsequently, we further detected the expression levels of CyclinD1 (a fibrosis growth factor), and Collagen I and Collagen III (ECM components) in keloid fibroblasts. As shown in Figure 2G, the downregulation of hsa_circ_0043688 could decrease the protein levels of CyclinD1, Collagen I, and Collagen III of keloid fibroblasts. Collectively, hsa_circ_0043688 silencing mitigated cell growth, metastasis, and ECM production of keloid fibroblasts.

3.3 | Hsa_circ_0043688 directly interacted with miR-145-5p in keloid fibroblasts

Considering cytoplasmic localization of hsa_circ_0043688 in keloid fibroblasts, we explored whether hsa_circ_0043688 exerted function in keloid by sponging miRNA. As shown in Figure 3A, through circular RNA Interactome software analysis, miR-145-5p is a candidate with the predicted binding site on hsa_circ_0043688. Meanwhile, miR-145-5p content was obviously blocked via a miR-145-5p mimic introduction (Figure 3B). After that, we further confirmed the binding, and the results suggested that the overexpression of miR-145-5p could significantly decline the luciferase activity of the WT-hsa_circ_0043688 reporter vector but not that of the MUT-hsa_circ_0043688 reporter vector in keloid fibroblasts using a dual-luciferase reporter assay (Figure 3C). Whereafter, RIP assay indicated hsa_circ_0043688

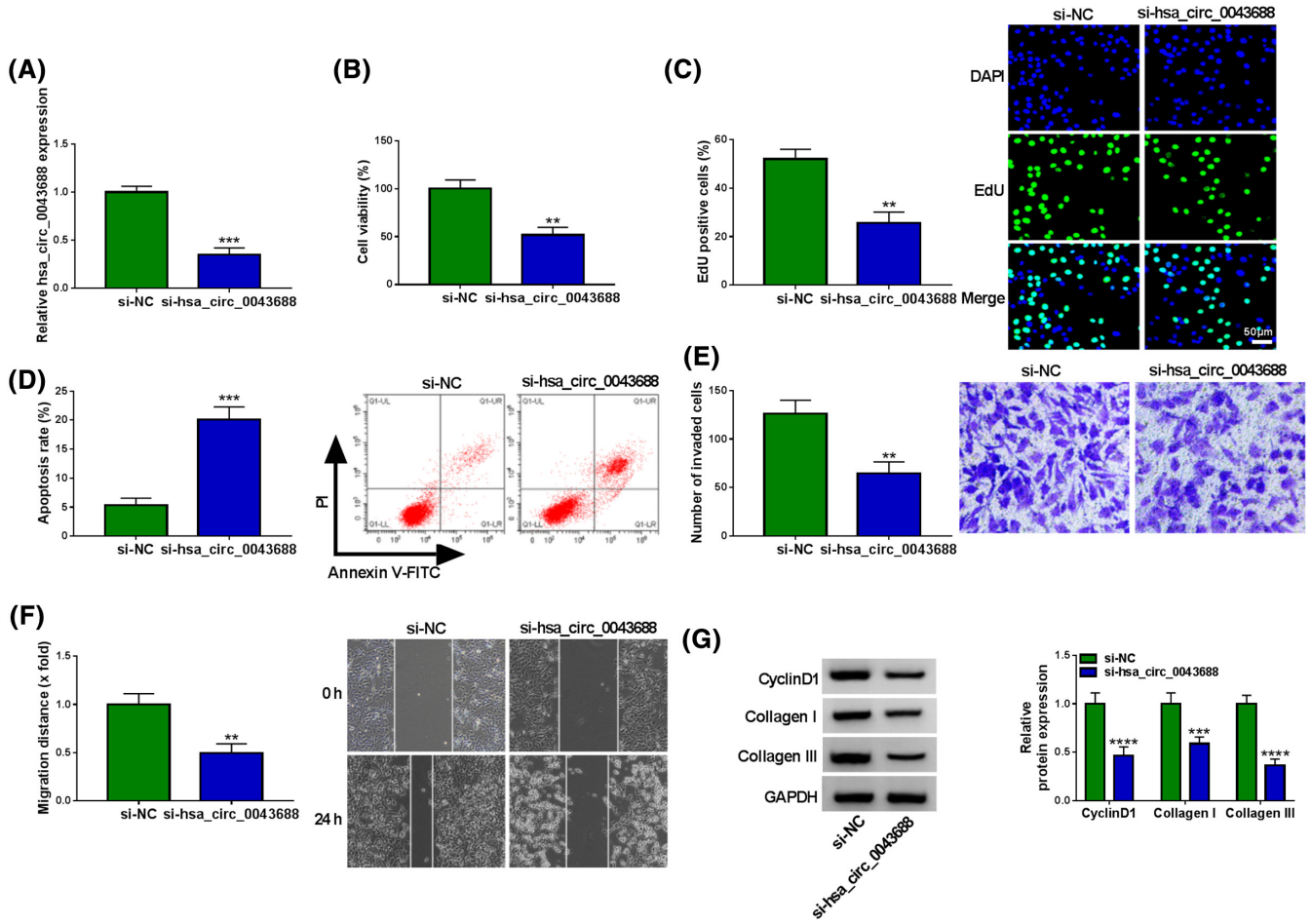

FIGURE 2 Effects of hsa_circ_0043688 downregulation on the malignant behavior of keloid fibroblasts. Keloid fibroblasts were transfected with si-NC or si-hsa_circ_0043688. (A) RT-qPCR analysis of hsa_circ_0043688 content in transfected keloid fibroblasts. (B and C) Cell proliferation was analyzed in transfected keloid fibroblasts by CCK-8 and EdU assay. (D) Apoptosis rates were examined in transfected keloid fibroblasts by flow cytometry assay. (E and F) Transwell and wound healing analysis of invasion and migration in transfected keloid fibroblasts. (G) Protein levels of CyclinD1, Collagen I, and Collagen III were determined in transfected keloid fibroblasts using western blot assay. $^{**}p < 0.01$, $^{***}p < 0.001$, $^{****}p < 0.0001$

and miR-145-5p were greatly enriched by anti-Ago2 in keloid fibroblast extracts (Figure 3D). Beyond that, miR-145-5p content was decreased in keloid tissues and cell lines (Figure 3E and G), inversely associated with hsa_circ_0043688 (Figure 3F). After being detected the overexpression efficiency of hsa_circ_0043688 in keloid fibroblasts (Figure 3H), miR-145-5p content was analyzed. As presented in Figure 3I, miR-145-5p was reinforced by hsa_circ_0043688 silencing, and was declined by hsa_circ_0043688 upregulation in keloid fibroblasts. All in all, circ_004368 negatively regulated miR-145-5p.

3.4 | Si-hsa_circ_0043688-mediated keloid fibroblasts phenotypes were abolished via miR-145-5p

Hsa_circ_0043688 absence hindered miR-145-5p content in keloid fibroblasts, where the influence was significantly counteracted via miR-145-5p knockdown (Figure 4A). Whereafter, functional analysis indicated that the inhibitory action of cell proliferation caused by hsa_circ_0043688 downregulation was overturned via anti-miR-145-5p in keloid fibroblasts (Figure 4B and C). What is more, hsa_circ_0043688 knockdown accelerated keloid fibroblasts apoptosis rate, which was significantly abrogated by miR-145-5p reduction (Figure 4D and E). Apart from that, hsa_circ_0043688 deficiency-mediated decline in invasion and migration in keloid fibroblasts was partly reversed via miR-145-5p inhibitor (Figure 4F and G). Additionally, decreased CyclinD1, Collagen I, and Collagen III via hsa_circ_0043688 knockdown were effectively ameliorated through miR-145-5p downregulation in keloid fibroblasts (Figure 4H). Together, hsa_circ_0043688 knockdown mitigated keloid fibroblasts phenotypes via targeting miR-145-5p.

3.5 | FGF2 was a direct target of miR-145-5p in keloid fibroblasts

Next, to understand the mechanisms of action of miR-145-5p, miR-145-5p targets in humans were identified. As shown in Figure 5A,

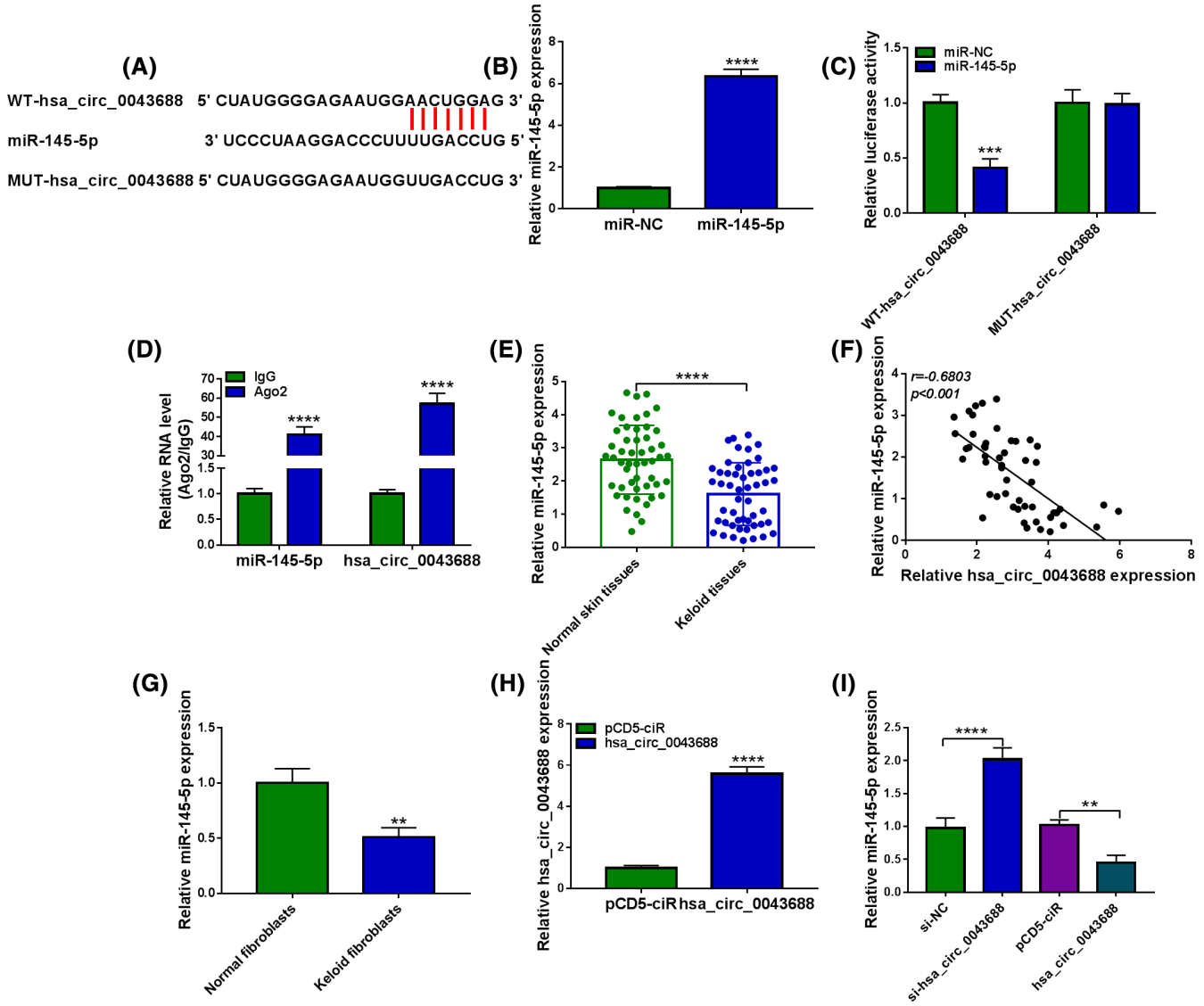

FIGURE 3 Hsa_circ_0043688 sequestered miR-145-5p in keloid fibroblasts. (A) The mutant and putative binding site of hsa_circ_0043688 with miR-145-5p. (B) miR-145-5p level was determined in miR-NC or miR-145-5p-transfected keloid fibroblasts by RT-qPCR assay. (C and D) Their binding was verified using a dual-luciferase reporter and RIP assay. (E) RT-qPCR analysis of miR-145-5p content keloid tissues. (F) The expression association between hsa_circ_0043688 and miR-145-5p in keloid tissues was analyzed by Pearson correlation analysis. (G) RT-qPCR analysis of miR-145-5p in keloid fibroblasts. (H) Hsa_circ_0043688 level was determined in pCD5-ciR or hsa_circ_0043688-transfected keloid fibroblasts by RT-qPCR assay. (I) Effects of hsa_circ_0043688 upregulation or silencing on miR-145-5p content were examined in keloid fibroblasts using RT-qPCR assay. $^{**}p < 0.01$, $^{****}p < 0.0001$

there were some binding sites between miR-145-5p and FGF2. Subsequent enhanced miR-145-5p resulted in a significant decline in the luciferase activity of WT-FGF2'UTR reporter in keloid fibroblasts (Figure 5B). Consistently, miR-145-5p and FGF2 of keloid fibroblasts were significantly enriched in the Ago2 group compared with the IgG group (Figure 5C). FGF2 content was improved in keloid tissues and negatively associated with miR-145-5p (Figure 5D and E). Also, the FGF2 protein level was elevated in keloid tissues and keloid fibroblasts when compared with the corresponding control group (Figure 5F and G). Whereafter, the introduction of anti-miR-145-5p apparently enhanced miR-145-5p content in Figure 5H. As expected, the FGF2 protein level was repressed via miR-145-5p overexpression in keloid fibroblasts, and improved on account of miR-145-5p down-regulation (Figure 5I). In a word, miR-145-5p directly targeted FGF2.

3.6 | miR-145-5p suppressed keloid-related phenotypes through interacting with FGF2

We next ascertained whether the increase in FGF2 levels might provide an explanation for the repression of keloid-associated phenotypes observed following miR-145-5p upregulation. As shown in Figure 6A, pcDNA-FGF2 re-introduction could significantly weaken miR-145-5p mimic-caused FGF2 decrease in keloid fibroblasts.

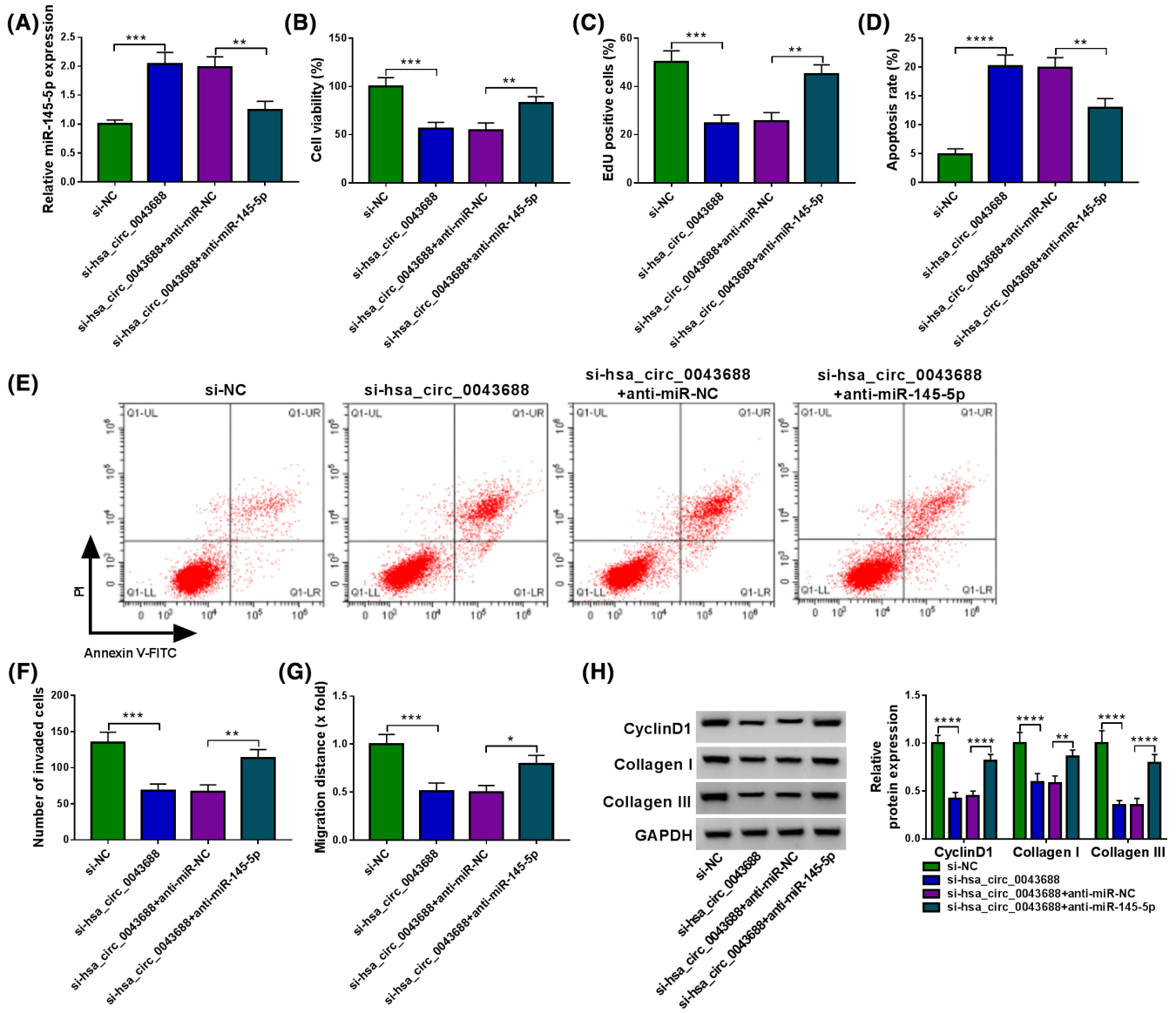

FIGURE 4 Effects of miR-145-5p on hsa_circ_0043688-regulated proliferation, apoptosis, invasion, and migration of keloid fibroblasts. Keloid fibroblasts were transfected with si-NC, si-hsa_circ_0043688, si-hsa_circ_0043688 + anti-miR-NC, and si-hsa_circ_0043688 + anti-miR-145-5p. (A) RT-qPCR analysis of miR-145-5p content in transfected keloid fibroblasts. (B and C) CCK-8 assay and EdU analysis of keloid fibroblasts proliferation ability. (D and E) Apoptosis rate in transfected keloid fibroblasts was assessed. (F and G) Transwell and wound healing assays were carried out to examine the capacities of invasion and migration in transfected keloid fibroblasts. (H) Western blot assay was conducted to test CyclinD1, Collagen I, and Collagen III protein levels in transfected keloid fibroblasts. $^{*}p < 0.05$, $^{**}p < 0.01$, $^{***}p < 0.001$, $^{****}p < 0.0001$

Functionally, overexpressed miR-145-5p could hamper the cell proliferation ability of keloid fibroblasts, while the co-transfection of FGF2 notably abolished the effect (Figure 6B and C), as evidenced by increased CyclinD1 (Figure 6H). Similarly, enhanced apoptosis rate (Figure 6D and E) and reduced the abilities of invasion and migration (Figure 6F and G) were noticed due to the upregulation of miR-145-5p, which was significantly overturned by pcDNA-FGF2 in keloid fibroblasts. In terms of ECM production, its primary constituents (Collagen I and Collagen III) were inhibited by miR-145-5p upregulation, and subsequently partly abrogated via FGF2 overexpression in keloid fibroblasts (Figure 6H). Overall, miR-145-5p relieved proliferation, metastasis, and ECM production by targeting FGF2 in keloid fibroblasts.

3.7 | Validation of hsa_circ_0043688/miR-145-5p/FGF2 regulatory axis in keloid fibroblasts

Based on the above findings, we interfered that hsa_circ_0043688 could exert the regulatory role by interacting with the miR-145-5p/FGF2 axis. To confirm the assumption, we carried out the rescue assays. As shown in Figure 7A and B, the knockdown of

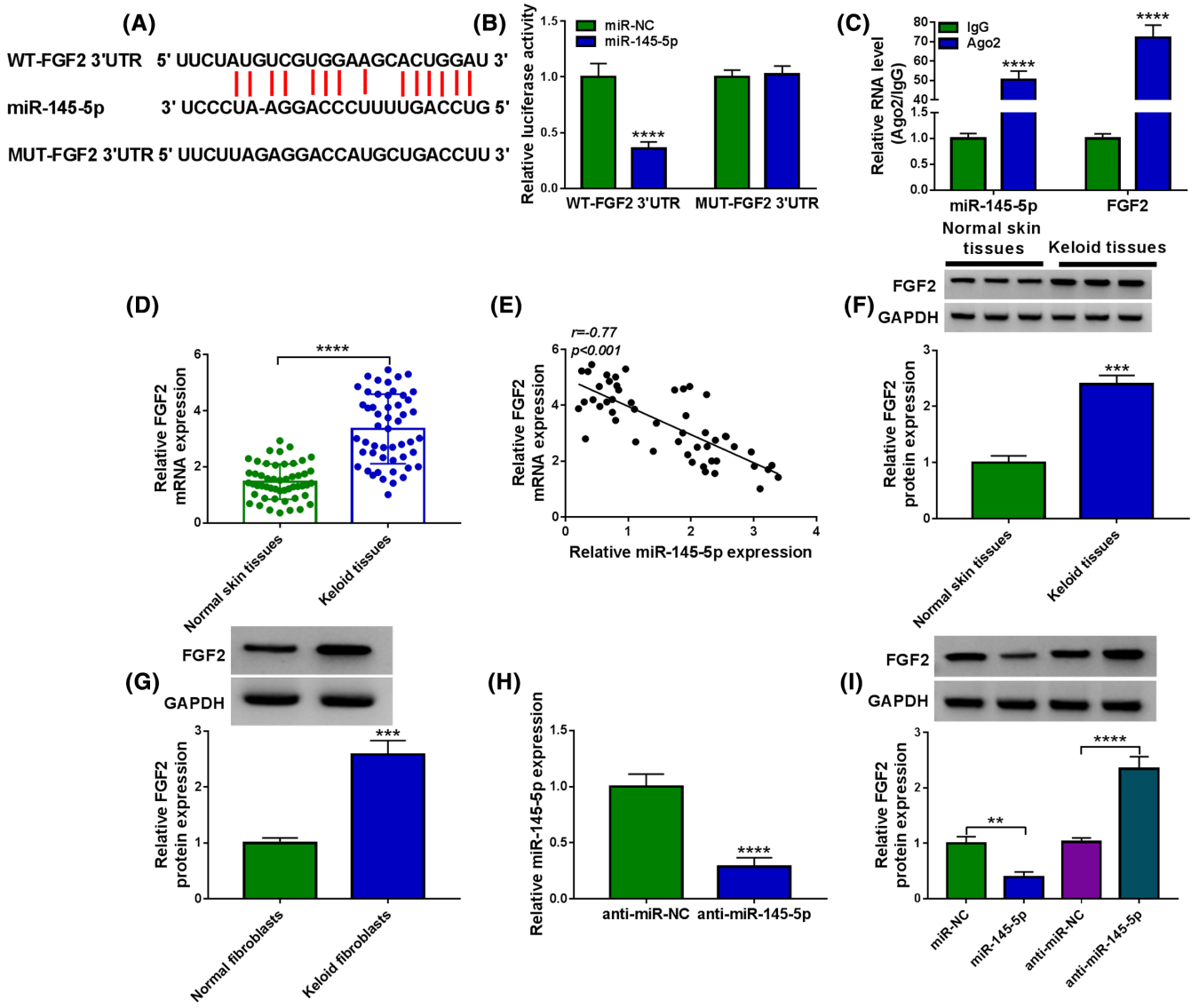

FIGURE 5 FGF2 acted as a target of miR-145-5p in keloid fibroblasts. (A) The sequences of FGF2 mRNA 3'UTR including wild type and mutant are shown with the miR-145-5p sequence. (B) A dual-luciferase reporter assay was used to examine the relative luciferase activity in keloid fibroblasts. (C) The endogenous association was analyzed by RIP assay. (D) FGF2 level was determined in normal skin tissues and keloid tissues by RT-qPCR assay. (E) Pearson correlation analysis was applied to evaluate the expression association between FGF2 and miR-145-5p in keloid tissues. (F) FGF2 protein level was examined in normal skin tissues and keloid tissues by western blot assay. (G) Western blot analysis of FGF2 protein level in normal fibroblasts and keloid fibroblasts. (H) Knockdown efficiency of anti-miR-145-5p in keloid fibroblasts was assessed. (I) FGF2 content was determined in keloid fibroblasts transfected with miR-NC, miR-145-5p, anti-miR-NC, and anti-miR-145-5p by western blot assay. $^{**}p < 0.01$, $^{***}p < 0.001$, $^{****}p < 0.0001$

hsa_circ_0043688 could decrease FGF2 expression, whereas the phenomenon was reversed via anti-miR-145-5p in keloid fibroblasts. These data implied hsa_circ_0043688 modulated FGF2 content via sponging miR-145-5p in keloid fibroblasts.

4 | DISCUSSION

During the past decades, circRNAs were initially reported sporadically and considered as the nonfunctional byproducts of splicing errors.[23] Intriguingly, an increasing number of circRNAs from various animal genomes have been gradually identified by the booming development of next-generation sequencing technology.[24,25] Unlike linear RNAs, most of them were highly stable and abundantly expressed, emphasizing the importance of underlying biomarkers in human diseases.[26,27] Virtually, it has been well-established that circRNAs were generally dysregulated in some diseases and participated in disease development. In terms of keloid, there is still limited knowledge about the role of circRNAs in disease progression in recent research.[28] In this work, the high expression of hsa_circ_0043688 was noticed in keloid tissues and fibroblasts, consistent with the former report.[19] Meanwhile,

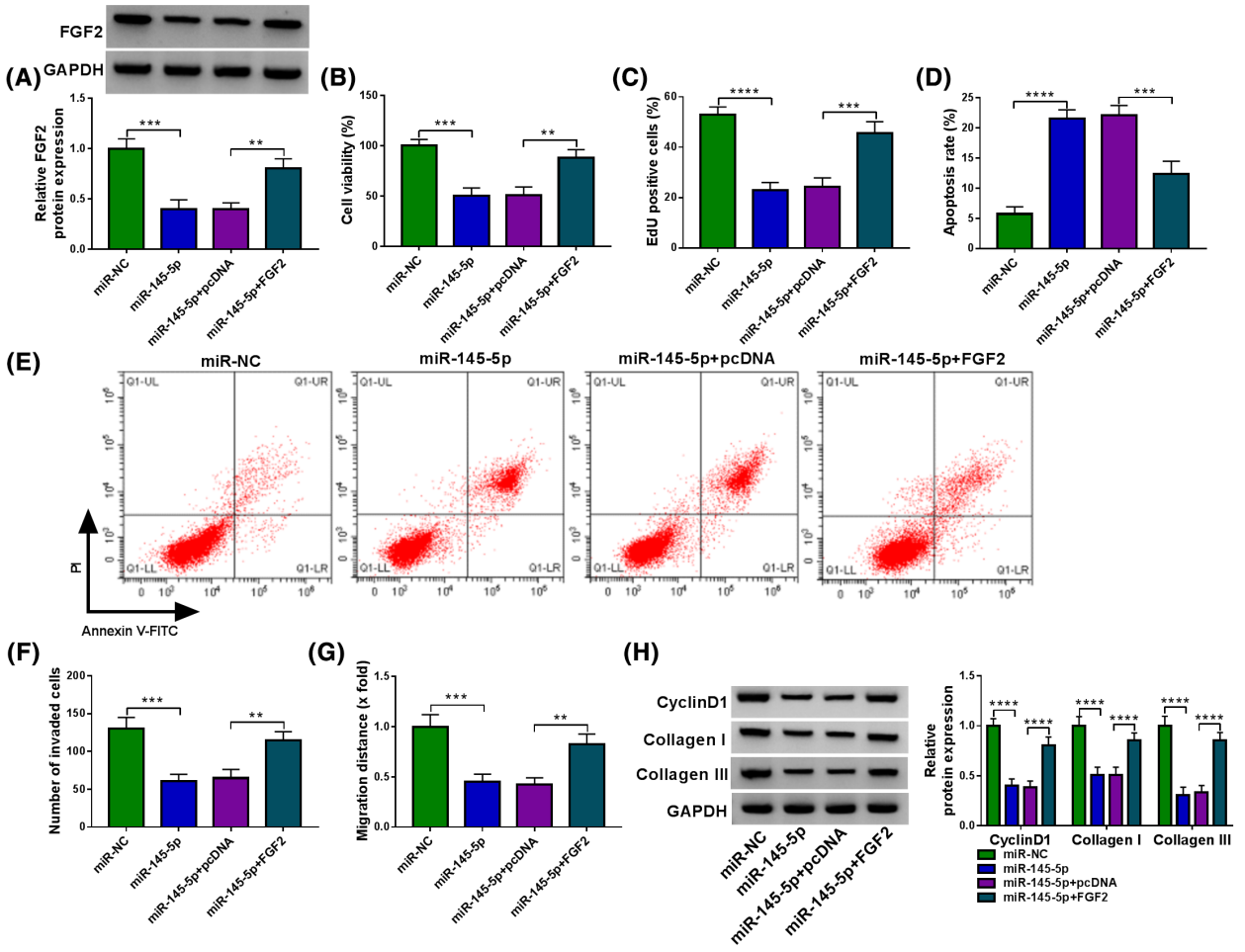

FIGURE 6 miR-145-5p inhibited proliferation, invasion, migration, and induced apoptosis of keloid fibroblasts by interacting with FGF2. Keloid fibroblasts were transfected with miR-NC, miR-145-5p, miR-145-5p + pcDNA, and miR-145-5p + FGF2. (A) Western blot analysis of FGF2 in transfected keloid fibroblasts. (B and C) The proliferation ability of keloid fibroblasts was analyzed by CCK-8 assay and EdU assay. (D and E) Apoptosis rate of keloid fibroblasts was assessed by flow cytometry assay. (F and G) The capacities of invasion and migration in keloid fibroblasts were examined by transwell and wound healing assay. (H) CyclinD1, Collagen I, and Collagen III protein levels of keloid fibroblasts were determined by RT-qPCR assay and western blot assay. $^{**}p < 0.01$, $^{***}p < 0.001$, $^{****}p < 0.0001$

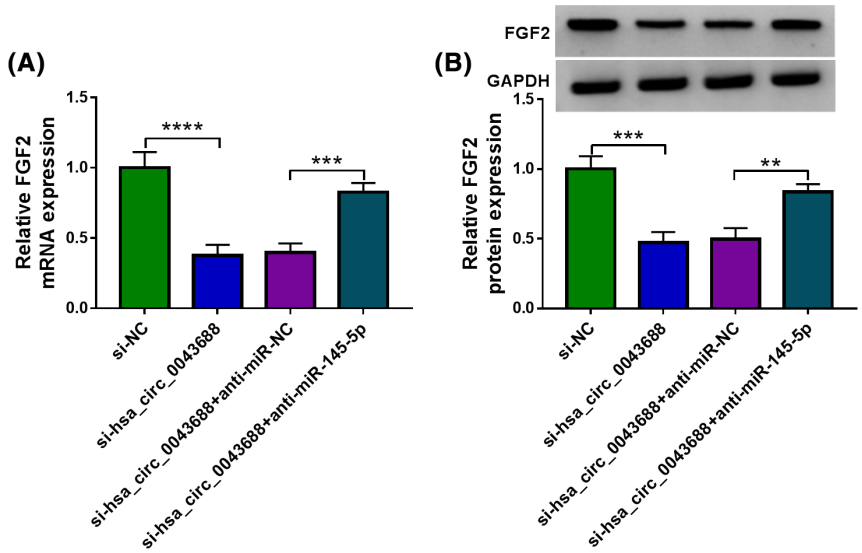

FIGURE 7 FGF2 was positively regulated by hsa_circ_0043688/miR-145-5p. (A and B) FGF2 level was detected in keloid fibroblasts transfected with si-NC, si-hsa_circ_0043688, si-hsa_circ_0043688 + anti-miR-NC, and si-hsa_circ_0043688 + anti-miR-145-5p by western blot assay. $^{**}p < 0.01$, $^{***}p < 0.001$, $^{****}p < 0.0001$

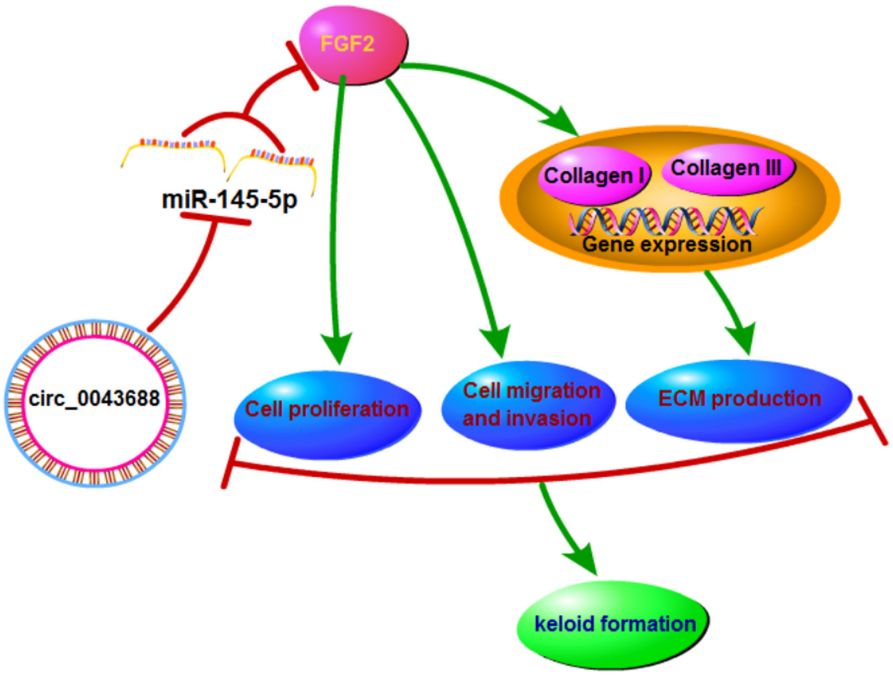

FIGURE 8 Hsa_circ_0043688 could regulate proliferation, migration, invasion, and ECM production of keloid fibroblasts by targeting the miR-145-5p/FGF2 axis

hsa_circ_0043688 was validated as a circular structure by RNase R treatment, suggesting a typical circRNA in keloid. Overall, hsa_circ_0043688 exerted a latent attractive biomarker in the keloid research.

Recent literature has described that uncontrolled fibroblast proliferation and invasiveness beyond surrounding skin are the overwhelming cause of keloid formation.[2,29] Combined with our results, hsa_circ_0043688 is likely to partake in keloid pathogenesis. In this work, hsa_circ_0043688 deficiency significantly hindered cell proliferation, invasion, migration, and induce apoptosis of keloid fibroblasts. Apart from that, another defining hallmark of keloid formation is excessive deposition of ECM components, particularly Collagen I and Collagen III.[30,31] In the paper, hsa_circ_0043688 downregulation repressed ECM production including Collagen I and Collagen III in keloid fibroblasts. That was to say, hsa_circ_0043688 might be involved in the pro-fibrotic process in keloid.

Several studies have stated that circRNAs mainly serve as efficient miRNA sponges in biological processes, thereby resulting in the depression of their target mRNAs. Furthermore, it has been reported that the cytoplasmic localization of circRNAs is related to miRNA sponging.[21,32] The current work identified underlying hsa_circ_0043688-interacting miRNAs. Considering the downregulation of miR-145-5p in keloid fibroblasts,[22] it was of particular interest in this current study. Also, our results highlight that hsa_circ_0043688 could directly target miR-145-5p for the first time. What is more, hsa_circ_0043688 silencing could attenuate the keloid formation by interacting with miR-145-5p. In this paper, we focused on FGF2, a basic fibroblast growth factor, which mediated the regulation of proliferation and metastasis.[33] Meanwhile, FGF2 has been confirmed to be correlated with the repair and healing processes in human keloid,[34] whose expression was upregulated in keloid fibroblasts.[35] In this research, miR-145-5p directly targeted FGF2. Synchronously, our data also proved elevated FGF2 partly mitigated miR-145-5p-induced keloid-related phenotypes suppression. Meanwhile, the inductive role of FGF2 elevation on cell viability, migration, and ECM expression of keloid fibroblasts was verified in the prior report.[36] More importantly, rescue assays proved that si-hsa_circ_0043688-caused decrease in FGF2 expression was in part overturned by miR-145-5p downregulation, further supporting the regulatory role of hsa_circ_0043688-miR-145-5p-FGF2 in the proliferation, invasion, and ECM expression of keloid fibroblasts (Figure 8).

5 | CONCLUSION

In summary, hsa_circ_0043688 was highly expressed in keloid tissue and cell lines, and its absence relieved keloid progression via the miR-145-5p/FGF2 axis. Accordingly, targeting of hsa_circ_0043688-governed singling network shed light on a prospective therapeutic target for this disease.

CONFLICT OF INTEREST

The authors declare that they have no conflicts of interest.

DATA AVAILABILITY STATEMENT

The data that support the findings of this study are available from the corresponding author upon reasonable request.

ORCID

Xiaojing li https://orcid.org/0000-0002-3282-6267

REFERENCES

1. Berman B, Maderal A, Raphael B. Keloids and hypertrophic scars: pathophysiology, classification, and treatment. *Dermatol Surg*. 2017;43(Suppl 1):S3-S18.
2. Limandjaja GC, Niessen FB, Scheper RJ, Gibbs S. The keloid disorder: heterogeneity, histopathology, mechanisms and models. *Front Cell Dev Biol*. 2020;8:360.
3. Mari W, Alsabri SG, Tabal N, et al. Novel insights on understanding of keloid scar: article review. *J Am Coll Clin Wound Spec*. 2015;7(1–3):1-7.
4. Jumper N, Paus R, Bayat A. Functional histopathology of keloid disease. *Histol Histopathol*. 2015;30(9):1033-1057.
5. Bijlard E, Kouwenberg CA, Timman R, et al. Burden of keloid disease: a cross-sectional health-related quality of life assessment. *Acta Derm Venereol*. 2017;97(2):225-229.
6. Lee HJ, Jang YJ. Recent understandings of biology, prophylaxis and treatment strategies for hypertrophic scars and keloids. *Int J Mol Sci*. 2018;19(3):711.
7. Ojeh N, Bharatha A, Gaur U, Forde AL. Keloids: Current and emerging therapies. *Scars Burn Heal*. 2020;6:2059513120940499.
8. Memariani H, Memariani M, Moravvej H, Shahidi-Dadras M. Emerging and novel therapies for keloids: a compendious review. *Sultan Qaboos Univ Med J*. 2021;21(1):e22-e33.
9. Birney E, Stamatoyannopoulos JA, Dutta A, et al. Identification and analysis of functional elements in 1% of the human genome by the ENCODE pilot project. *Nature*. 2007;447(7146):799-816.
10. Hombach S, Kretz M. Non-coding RNAs: classification, biology and functioning. *Adv Exp Med Biol*. 2016;937:3-17.
11. Lu Y, Li Z, Lin C, Zhang J, Shen Z. Translation role of circRNAs in cancers. *J Clin Lab Anal*. 2021;35(7):e23866.
12. Kristensen LS, Andersen MS, Stagsted LVW, et al. The biogenesis, biology and characterization of circular RNAs. *Nat Rev Genet*. 2019;20(11):675-691.
13. Ashwal-Fluss R, Meyer M, Pamudurti NR, et al. circRNA biogenesis competes with pre-mRNA splicing. *Mol Cell*. 2014;56(1):55-66.
14. Zhang Z, Yang T, Xiao J. Circular RNAs: promising biomarkers for human diseases. *EBio Med*. 2018;34:267-274.
15. Liu L, Wang J, Khanabdali R, et al. Circular RNAs: isolation, characterization and their potential role in diseases. *RNA Biol*. 2017;14(12):1715-1721.
16. Wang J, Wu H, Xiao Z, Dong X. Expression Profiles of lncRNAs and circRNAs in Keloid. *Plast Reconstr Surg Glob Open*. 2019;7(6):e2265.
17. Lv W, Liu S, Zhang Q, et al. Circular RNA CircCOL5A1 sponges the MiR-7-5p/epac1 axis to promote the progression of keloids through regulating PI3K/Akt signaling pathway. *Front Cell Dev Biol*. 2021;9:626027.
18. Yang D, Li M, Du N. Effects of the circ_101238/miR-138-5p/CDK6 axis on proliferation and apoptosis keloid fibroblasts. *Exp Ther Med*. 2020;20(3):1995-2002.
19. Shi J, Yao S, Chen P, et al. The integrative regulatory network of circRNA and microRNA in keloid scarring. *Mol Biol Rep*. 2020;47(1):201-209.
20. Panda AC. Circular RNAs Act as miRNA Sponges. *Adv Exp Med Biol*. 2018;1087:67-79.
21. Hansen TB, Jensen TI, Clausen BH, et al. Natural RNA circles function as efficient microRNA sponges. *Nature*. 2013;495(7441):384-388.
22. Li C, Bai Y, Liu H, et al. Comparative study of microRNA profiling in keloid fibroblast and annotation of differential expressed microRNAs. *Acta Biochim Biophys Sin*. 2013;45(8):692-699.
23. Jeck WR, Sharpless NE. Detecting and characterizing circular RNAs. *Nat Biotechnol*. 2014;32(5):453-461.
24. López-Jiménez E, Rojas AM, Andrés-León E. RNA sequencing and prediction tools for circular RNAs analysis. *Adv Exp Med Biol*. 2018;1087:17-33.
25. Sekar S, Geiger P, Cuyugan L, et al. Identification of Circular RNAs using RNA Sequencing. *J Vis Exp*. 2019. doi:10.3791/59981
26. Santer L, Bär C, Thum T. Circular RNAs: a novel class of functional rna molecules with a therapeutic perspective. *Mol Ther*. 2019;27(8):1350-1363.
27. Han B, Chao J, Yao H. Circular RNA and its mechanisms in disease: from the bench to the clinic. *Pharmacol Ther*. 2018;187:31-44.
28. Zhang Z, Yu K, Liu O, et al. Expression profile and bioinformatics analyses of circular RNAs in keloid and normal dermal fibroblasts. *Exp Cell Res*. 2020;388(1):111799.
29. Andrews JP, Marttala J, Macarak E, Rosenbloom J, Uitto J. Keloids: the paradigm of skin fibrosis - pathomechanisms and treatment. *Matrix Biol*. 2016;51:37-46.
30. Chong Y, Park TH, Seo S, Chang CH. Histomorphometric analysis of collagen architecture of auricular keloids in an Asian population. *Dermatol Surg*. 2015;41(3):415-422.
31. Kashiyama K, Mitsutake N, Matsuse M, et al. miR-196a downregulation increases the expression of type I and III collagens in keloid fibroblasts. *J Invest Dermatol*. 2012;132(6):1597-1604.
32. Chen LL. The biogenesis and emerging roles of circular RNAs. *Nat Rev Mol Cell Biol*. 2016;17(4):205-211.
33. Shi H, Xu J, Zhao R, et al. FGF2 regulates proliferation, migration, and invasion of ECA109 cells through PI3K/Akt signalling pathway in vitro. *Cell Biol Int*. 2016;40(5):524-533.
34. Sideek MA, Teia A, Kopecki Z, Cowin AJ, Gibson MA. Co-localization of LTBP-2 with FGF-2 in fibrotic human keloid and hypertrophic scar. *J Mol Histol*. 2016;47(1):35-45.
35. Shi K, Qiu X, Zheng W, Yan D, Peng W. MiR-203 regulates keloid fibroblast proliferation, invasion, and extracellular matrix expression by targeting EGR1 and FGF2. *Biomed Pharmacother*. 2018;108:1282-1288.
36. Yang J, Deng P, Qi Y, et al. NEAT1 knockdown inhibits keloid fibroblast progression by miR-196b-5p/FGF2 Axis. *J Surg Res*. 2021;259:261-270.

How to cite this article: Liu Y, Wang X, Ni Z, et al.. Circular RNA hsa_circ_0043688 serves as a competing endogenous RNA for microRNA-145-5p to promote the progression of Keloids via Fibroblast growth factor-2. *J Clin Lab Anal*. 2022;36:e24528. doi: 10.1002/jcla.24528